



Published in final edited form as:

*J Urol.* 2015 January ; 193(1): 338–344. doi:10.1016/j.juro.2014.08.009.

## FRAGMENTATION OF URINARY CALCULI *IN VITRO* BY BURST WAVE LITHOTRIPSY

Adam D. Maxwell<sup>1,2</sup>, Bryan W. Cunitz<sup>2</sup>, Wayne Kreider<sup>2</sup>, Oleg A. Sapozhnikov<sup>2,3</sup>, Ryan S. Hsi<sup>1</sup>, Jonathan D. Harper<sup>1</sup>, Michael R. Bailey<sup>2</sup>, and Mathew D. Sorensen<sup>1,4</sup>

<sup>1</sup>Department of Urology, University of Washington School of Medicine, 1959 NE Pacific Street, Box 356510, Seattle, WA 98195

<sup>2</sup>Center for Industrial and Medical Ultrasound, Applied Physics Laboratory, University of Washington, 1013 NE 40<sup>th</sup> Street, Seattle, WA 98105

<sup>3</sup>Department of Acoustics, Physics Faculty, Moscow State University, Leninskie Gory, Moscow, Russia 119991

<sup>4</sup>Division of Urology, Department of Veteran Affairs Medical Center, 1660 S Columbian Way, Seattle, WA 98108

### Abstract

**Purpose**—We have developed a new method of lithotripsy that uses short, broadly focused bursts of ultrasound rather than shock waves to fragment stones. This study investigated the characteristics of stone comminution by burst wave lithotripsy *in vitro*.

**Materials and Methods**—Artificial and natural stones (mean 8.2±3.0 mm, range 5–15 mm) were treated with ultrasound bursts using a focused transducer in a water bath. Stones were exposed to bursts with focal pressure amplitude 6.5 MPa at 200 Hz burst repetition rate until completely fragmented. Ultrasound frequencies of 170 kHz, 285 kHz, and 800 kHz were applied using 3 different transducers. The time to achieve fragmentation for each stone type was recorded, and fragment size distribution was measured by sieving.

**Results**—Stones exposed to ultrasound bursts were fragmented at focal pressure amplitudes 2.8 MPa at 170 kHz. Fractures appeared along the stone surface, resulting in fragments separating at the surface nearest to the transducer until the stone was disintegrated. All natural and artificial stones were fragmented at the highest focal pressure of 6.5 MPa with treatment durations between a mean of 36 seconds for uric acid to 14.7 minutes for cystine stones. At a frequency of 170 kHz, the largest artificial stone fragments were <4 mm. Exposures at 285 kHz produced only fragments <2 mm, and 800 kHz produced only fragments <1 mm.

**Conclusions**—Stone comminution with burst wave lithotripsy is feasible as a potential noninvasive treatment method for nephrolithiasis. Adjusting the fundamental ultrasound frequency allows control of stone fragment size.

## Keywords

Extracorporeal Shock Wave Lithotripsy; Ultrasonic Lithotripsy; Ultrasonic Therapy; Urinary Stone

---

## INTRODUCTION

Surgical management of urolithiasis has changed significantly since the introduction of shock wave lithotripsy (SWL) in the early 1980's<sup>1,2,3,4</sup>. This technology, along with the development of endoscopic techniques such as ureteroscopy<sup>5</sup> and percutaneous nephrolithotomy<sup>6,7</sup> have almost completely replaced open surgery as a treatment option<sup>8,9</sup>. While minimally invasive methods continue to be refined, SWL remains the only extracorporeal procedure for stone disintegration.

Despite the discovery of shock wave-induced stone fracture almost 40 years ago, the acoustic output of lithotripters remains similar to the original implementation. Newer lithotripters exhibit different focal dimensions and pressures, but all systems deliver single-shock waveforms at a rate of 1–2 Hz with a maximal dose of approximately 2500–3000 shocks. Several studies indicate that the first lithotripter used in clinical practice in the United States, the Dornier HM3, is more effective than many of its newer counterparts<sup>10,11</sup>. These revelations have in turn led to production of several machines with similar specifications to the HM3, delivering broadly focused shocks with relatively low pressure amplitudes<sup>12</sup>. Investigations into the physical mechanisms of lithotripsy also support a broad-focus, low-pressure configuration as more effective in achieving stone comminution<sup>13,14,15</sup>. While there have been advancements toward achieving a more ideal lithotripter, the low effectiveness reported with many systems has led to greater clinical preference toward endoscopic techniques<sup>16</sup>.

To expand on the capabilities of SWL as an extracorporeal treatment, ultrasound-based alternatives have been explored<sup>17,18</sup>. In previous work, pulses of high intensity focused ultrasound (HIFU) have been strongly focused onto the stone surface to generate a localized cloud of cavitation bubbles, whereby the associated bubble collapses against the stone surface can erode it into very fine dust. Heating of the surrounding tissue, as observed in HIFU thermal therapy, is avoided by pulsing the ultrasound with sufficiently low duty cycle.

Here, we also explore the use of focused ultrasound to break stones; however, we employ a beam that is broadly focused to a width similar to or greater than the stone in order to excite elastic waves in the stone that produce discrete fragments rather than dust-like particles. This technique applies sinusoidal ultrasound bursts with relatively low pressure amplitudes rather than shock waves (Figure 1) to prevent accumulation of cavitation bubbles that shield acoustic waves from propagating into the stone and causing fracture<sup>19</sup>. Similar to SWL, burst wave lithotripsy (BWL) uses a focused source to generate pressure pulses that can be transcutaneously administered. The purpose of this study was to examine the feasibility of stone fracture by BWL applied to both artificial and natural calculi *in vitro*.

## MATERIALS AND METHODS

### Artificial and Natural Stone Preparation

Artificial stones were created using a model developed by Liu and Zhong<sup>20</sup>, which have acoustic properties similar to natural calcium oxalate monohydrate (COM) stones. Begostone plaster powder was mixed with deionized, degassed water in a ratio of 5:1 by weight. Aliquots of the mixture were then pipetted into an acetal plastic mold to form cylindrical stones of 6 mm diameter and 10–12 mm length. The mold was placed in a water bath 30 minutes after pipetting and allowed to further set for at least 12 hours. The stones were then removed from the mold and placed in deionized water until use in the experiments.

Human stones with primary compositions (>90%, spectroscopic analysis by Beck Analytical Laboratories, Greenwood, IN) of uric acid, magnesium ammonium phosphate (struvite), COM, and cystine were also obtained for experiments. The largest dimension of each stone was between 5 – 15 mm (mean 8.2+/-3.0 mm). The stones were submerged in deionized water at least 72 hours prior to experiments.

### Burst Wave Lithotripsy System

Exposures were performed using three piezoelectric focused ultrasound transducers with operating frequencies of 170 kHz, 285 kHz, and 800 kHz. The transducers were driven by a high-voltage radiofrequency amplifier<sup>21</sup> controlled with a field-programmable gate array board (DE1, Altera, San Jose, CA, USA). Each transducer was calibrated using a fiber optic hydrophone (FOPH2000, RP Acoustics, Leutenbach, Germany) to measure the pressure waveforms in the focal region and effective beamwidth in a degassed water bath. The focus of each ultrasound transducer was defined by an ellipsoidal region of high pressure amplitude. The aperture, focal length, and focal beam dimensions of the three transducers are given in Table 1. Because the focal dimensions of the transducer differ significantly, the stones were aligned in a prefocal position when using the 285 kHz and 800 kHz transducers to match the beamwidth of the 170 kHz transducer. The pressure output of each transducer was then adjusted such that the peak pressure amplitude in the plane aligned with the stone center was virtually the same for all three devices. This was done in order to facilitate an even comparison between different frequencies by treating stones using the same beamwidth and pressure amplitude of burst at all three frequencies.

### Stone Exposures

The transducer was positioned in a bath of filtered water that was degassed to approximately 20% O<sub>2</sub> saturation (Figure 1c). A small amount of cyanoacrylate adhesive was used to affix the stone to a 25- $\mu$ m thick acoustically transparent polyester membrane attached over a polyvinyl chloride plastic hoop. This apparatus held the stone in a stable position during treatment to observe the progression of fragmentation and minimized reflections from the holder. The stone and holder were attached to a motorized, 3-axis positioning system (Velmex, Inc, Bloomfield, NY, USA) that allowed precise alignment of the stone with the focus. A digital camera was used to record images of stones and fragments before, during, and after acoustic exposure. Stones were exposed to ultrasound bursts with duration of 10

cycles and focal pressure amplitude  $p_f = 6.5$  MPa. The number of bursts administered per second (burst repetition rate) was fixed at 200 Hz. Note that the burst repetition rate is a separate parameter from the ultrasound frequency (which determines the rate of oscillations within a single burst). After treatment, stone fragments that dropped into a basket were collected and allowed to dry, then photographed and passed through a series of sieves to determine the fragment size distribution.

Several experiments were performed to evaluate the *in vitro* characteristics of stone fragmentation by BWL (Table 2). First, to determine the pressure threshold for stone fragmentation artificial stones were treated for 5 minutes each at different pressure amplitudes ( $n = 3$  per amplitude,  $p_f = 1.2$  to 6.5 MPa) at 170 kHz. Second, to determine the effect of stone composition on stone fragmentation, both artificial ( $n = 12$ ) and natural stones ( $n = 3$  per composition) were exposed to the highest pressure amplitude ( $p_f = 6.5$  MPa) and the resulting exposure times and fragment size distribution were compared. Finally, to evaluate the effect of the ultrasound frequency on fragment size, artificial stones were exposed to ultrasound frequencies of 170 kHz, 285 kHz, and 800 kHz.

## RESULTS

Erosion and multiple fractures were observed in stones treated at 170 kHz for focal pressure amplitudes  $p_f = 2.8$  MPa (Figure 2). At the next lowest pressure amplitude ( $p_f = 2.3$  MPa) and below, no change in the stones was visible over the exposure duration of 5 minutes (60,000 bursts). Above  $p_f = 2.3$  MPa, very fine dust was emitted from the stone, and fracture lines were observed on its surface, predominantly aligned along the circumferential and longitudinal directions of the cylindrical stone. Subsequently, fragments separated from the stone, with the fragment geometry resulting from the location of these fractures. Fragmentation generally initiated at the surface of the stone nearest the transducer and proceeded distally.

In the second series of experiments, all artificial stones and natural stones of four different compositions exposed to 170 kHz bursts at the highest pressure amplitude ( $p_f = 6.5$  MPa) were successfully fragmented (Figures 3,4). In these trials, the entire stone was disintegrated with the exception of a small portion directly adhered to the membrane (Figure 3). The artificial stones treated at a pressure amplitude  $p_f = 6.5$  MPa ( $n = 12$ ) required  $9.7 \pm 2.8$  minutes (mean  $\pm$  SD) to achieve complete fragmentation. The progression of treatment and resulting fragmentation of natural stones proceeded similarly to that observed with the artificial stones. However, the time required to achieve fragmentation varied greatly with stone type. For instance, a 7-mm struvite stone could be fragmented in 4 seconds (800 bursts), while a similarly sized cystine stone required 10.3 minutes (123,600 bursts). The range of treatment times was 0.17–1.40 minutes for uric acid, 0.07 – 2.02 minutes for struvite, 8.0 – 18.1 minutes for COM, and 10.3 – 21.3 minutes for cystine stones.

The sizes of fragments produced by each treatment were consistent among stones of the same composition. Figure 5 shows the distribution of the collected fragments as a proportion of the total mass, obtained by sequential sieving. While variations in the distribution of fragment sizes can be seen between different stone types, the largest fragments produced for

each type were similar in size. None of the treatments produced fragments >4mm. The largest fragments were 3–4 mm for COM, uric acid, and artificial stones, and 2–3 mm for struvite and cystine stones. A majority of the fragment mass was <3 mm for COM and uric acid, <2 mm for artificial, and <1 mm for struvite and cystine stones.

In the third experiment, artificial stones treated with exposures at three different frequencies were compared. At 170 kHz, circumferential fractures in the stone appeared evenly spaced (approximately 3 mm apart along the length of the cylinder) and did not appear to change in density with pressure amplitude. Exposures at 285 kHz and 800 kHz produced more closely spaced fractures in the stone, and resulted in smaller fragments compared with treatments at 170 kHz (Figures 5 and 6). At 285 kHz, no fragments larger than 2 mm were generated, and at 800 kHz, no fragments larger than 1 mm were generated.

## DISCUSSION

SWL has been the sole extracorporeal therapy for renal stones for more than 30 years. While the physical mechanisms of shock wave-induced stone fracture were not fully understood during its clinical introduction, subsequent research has identified two particularly important effects: elastic waves within the stone and cavitation at the stone surface<sup>14,15,22</sup>. Regarding the first, shear waves appear to be a dominant mechanism when using a focus broader than the stone, causing tension that leads to growth of fractures and fragmentation<sup>15,23</sup>. Second, shock-induced cavitation at the stone surface can initiate these fractures<sup>13,16</sup>. At the same time, proliferation of cavitation clouds caused by delivering shocks at too great of a rate tends to reduce their effectiveness<sup>19</sup> and can lead to tissue damage<sup>24</sup>. In the present study, we employed bursts that were broadly focused to generate shear, and sought to avoid cavitation clouds by using relatively low-pressure pulses that could be delivered at a fast repetition rate to maximize the energy transferred into the stone. Provided such bursts produce the necessary tension within the stone to generate and propagate fractures, a shocked waveform is not required to produce comminution.

Another technique using focused ultrasound has also been reported, but takes an alternate approach relying solely on acoustic cavitation<sup>17,18</sup>. While the cloud of bubbles likely reduces propagation of acoustic energy into the stone, cavitation collapses against its surface can reduce it to very fine dust through surface erosion without generating the deep fractures we observed. While this technique has not yet been demonstrated *in vivo*, it may also provide a noninvasive therapeutic alternative to SWL.

Our results demonstrate that broadly focused burst waves are capable of fracturing stones of varying composition, including some considered to be resistant to SWL such as cystine<sup>25,26</sup>. While we did not measure the threshold to fragment natural calculi, artificial stones could be treated at focal pressures as low as 2.8 MPa. This level is at least an order of magnitude lower than shock amplitudes for SWL in practice (30–100 MPa), although it has also been demonstrated by Eisenmenger that fracture of artificial stones can be accomplished with shock amplitudes as low as 11 MPa<sup>27</sup>. Though lower pressure amplitudes were applied in our study, bursts were administered at a much greater rate (200 Hz) than a typical SWL pulse repetition rate (1–2 Hz). The result of this rapid delivery of energy to the stone is

evident particularly with the softer stone compositions (uric acid and struvite), which underwent fragmentation in only a few seconds in some experiments. COM and cystine stones required longer exposures, but all treatments achieved complete comminution of the stones into clinically passable fragments (< 4 mm). While current practice applies a fairly consistent dose of shock waves (2000–3000 per session), these results suggest that different stone types require greatly varying energy to disintegrate, and feedback on treatment progression could be valuable in efficiently achieving a therapeutic endpoint.

One notable advantage of this form of therapy over SWL may be the ability to control the size of the fragments, which is clinically relevant to produce stone fragments with a high likelihood of spontaneous passage through the urinary tract. Treatments with a 170 kHz transducer produced fragments of similar size for different stone types, with maximum fragment sizes of ~3 mm. Studies exposing stones at three different frequencies suggested that higher frequencies generate more densely-spaced fractures, resulting in smaller fragments. Our preliminary simulations and experiments suggest that bursts between 400–500 kHz would generate fragments ~1 mm maximum, which might be clinically ideal.

While optimizing stone fragmentation may be achievable through such experimentation, it must also be carefully weighed against the effect of the particular burst parameters on the surrounding kidney tissue. SWL is known to cause parenchymal injury to kidney tissue<sup>24,28</sup>, and the type and severity of lesions can vary with different lithotripters<sup>29,30</sup>. It is possible that mechanical hemorrhagic injury could result from cavitation in BWL when the pressure amplitude or PRF is too high, similar to SWL. The heating due to ultrasound is minimized because of the low frequency and low spatial-peak temporal-average intensity (~15 W/cm<sup>2</sup>), thus it is not expected that thermal injury such as that found with HIFU thermal therapy will result with the parameters used in this study. We did not evaluate kidney injury in this study, and BWL will require a separate investigation in an *in vivo* model to accurately assess the acute and long-term effects of the exposures. In addition to evaluation of injury, further tests are needed to assess the characteristics of stone fragmentation under clinically-relevant conditions. The *in vitro* experimental setup used here performed exposures on fixed stones in a specific orientation. While this allowed us to examine the repeatable characteristics of stone fracture, a free stone would more accurately simulate a physiologic situation. The fragments did not remain in the focus for the duration of treatment, but rather fell out after separation from the stone. It could be argued that these fragments would be further reduced in size had they remained in or near the focus for the treatment duration. Another limitation of this preliminary study was that several of the burst parameters were necessarily fixed. Future work should explore the effects of changing parameters such as burst length, burst repetition rate, and amplitude, guided by theoretical and experimental analysis of the physical mechanisms.

## CONCLUSIONS

This study demonstrated the feasibility of fragmenting urinary calculi using broadly focused ultrasound bursts. Bursts were observed to produce fractures in artificial and human calculi that led to fragmentation of all stone types. The duration of exposure required to reduce stones to passable fragments varied with stone type. The size of the resultant stone

fragments could be controlled by adjusting ultrasound frequency. These characteristics suggest BWL may offer a potentially viable noninvasive alternative to SWL.

## Acknowledgments

The authors wish to thank Prof. James Williams from Indiana University-Purdue University Indianapolis for providing the natural stones for experiments. This work was supported by the National Institute of Health through 2T32 DK007779-11A1, 2R01 EB007643-05, P01 DK043881, and R01 DK092197, and by NSBRI through NASA NCC 9-58.

## References

1. Bandi G, Best SL, Nakada SY. Current practice patterns in the management of upper urinary tract calculi in the north central United States. *J Endourol.* 2008; 22:631–636. [PubMed: 18366318]
2. Bird VG, Fallon B, Winfield HN. Practice patterns in the treatment of large renal stones. *J Endourol.* 2003; 17:355–363. [PubMed: 12965059]
3. Matlaga BR. Contemporary surgical management of upper urinary tract calculi. *J Urol.* 2009; 181:2152–2156. [PubMed: 19296977]
4. Chaussy C, Schmiedt E, Jocham D, et al. First clinical experience with extracorporeally induced destruction of kidney stones by shock waves. *J Urol.* 1982; 127:417–420. [PubMed: 6977650]
5. Payne SR, Ford TF, Wickham JE. Endoscopic management of upper urinary tract stones. *Br J Surg.* 1985; 72:822–824. [PubMed: 4041714]
6. Clayman RV, Surya V, Miller RP, et al. Percutaneous nephrolithotomy: Extraction of renal and ureteral calculi from 100 patients. *J Urol.* 1984; 131:868–871. [PubMed: 6708216]
7. Wickham JE, Kellett MJ. Percutaneous nephrolithotomy. *Br J Urol.* 1981; 53:297–299. [PubMed: 7260539]
8. Paik ML, Wainstein MA, Spirnak JP, et al. Current indications for open stone surgery in the treatment of renal and ureteral calculi. *J Urol.* 1998; 159:374–378. [PubMed: 9649242]
9. Matlaga BR, Assimos DG. Changing indications of open stone surgery. *Urology.* 2002; 59:490–493. [PubMed: 11927296]
10. Gerber R, Studer UE, Danuser H. Is newer always better? A comparative study of 3 lithotripter generations. *J Urol.* 2005; 173:2013–2016. [PubMed: 15879807]
11. Teichman JM, Portis AJ, Cecconi PP, et al. In vitro comparison of shock wave lithotripsy machines. *J Urol.* 2000; 164:1259–1264. [PubMed: 10992376]
12. Eisenmenger W, Du XX, Tang C, et al. The first clinical results of “wide-focus and low-pressure” ESWL. *Ultrasound Med Biol.* 2002; 28:769–774. [PubMed: 12113789]
13. Howard D, Sturtevant B. In vitro study of the mechanical effects of shock-wave lithotripsy. *Ultrasound Med Biol.* 1997; 23:1107–1122. [PubMed: 9330454]
14. Zhu S, Cocks FH, Preminger GM, et al. The role of stress waves and cavitation in stone comminution in shock wave lithotripsy. *Ultrasound Med Biol.* 2002; 28:661–671. [PubMed: 12079703]
15. Sapozhnikov OA, Maxwell AD, MacConaghy B, et al. A mechanistic analysis of stone fracture in lithotripsy. *J Acoust Soc Am.* 2007; 121:1190–1202. [PubMed: 17348540]
16. Kerbl K, Rehman J, Landman J, et al. Current management of urolithiasis: Progress or regress? *J Endourol.* 2002; 16:281–288. [PubMed: 12184077]
17. Ikeda T, Yoshizawa S, Tosaki M, et al. Cloud cavitation control for lithotripsy using high intensity focused ultrasound. *Ultrasound Med Biol.* 2006; 32:1383–1397. [PubMed: 16965979]
18. Duryea AP, Hall TL, Maxwell AD, et al. Histotripsy erosion of model urinary calculi. *J Endourol.* 2011; 25:341–344. [PubMed: 21091223]
19. Pishchalnikov YA, McAteer JA, Williams JC Jr, et al. Why stones break better at slow shockwave rates than at fast rates: In vitro study with a research electrohydraulic lithotripter. *J Endourol.* 2006; 20:537–541. [PubMed: 16903810]

20. Liu Y, Zhong P. Begostone--a new stone phantom for shock wave lithotripsy research. *J Acoust Soc Am.* 2002; 112:1265–1268. [PubMed: 12398432]
21. Hall, TL.; Cain, CA. A low cost, compact, 512 channel therapeutic system for transcutaneous ultrasound surgery. *AIP Conf Proc; International Symposium on Therapeutic Ultrasound; Boston, USA.* 2006. p. 445-449.
22. Rassweiler JJ, Knoll T, Kohrmann KU, et al. Shock wave technology and application: An update. *Eur Urol.* 2011; 59:784–796. [PubMed: 21354696]
23. Cleveland RO, Sapozhnikov OA. Modeling elastic wave propagation in kidney stones with application to shock wave lithotripsy. *J Acoust Soc Am.* 2005; 118:2667–2676. [PubMed: 16266186]
24. Blomgren PM, Connors BA, Lingeman JE, et al. Quantitation of shock wave lithotripsy-induced lesion in small and large pig kidneys. *Anat Rec.* 1997; 249:341–348. [PubMed: 9372167]
25. Strem SB. Contemporary clinical practice of shock wave lithotripsy: A reevaluation of contraindications. *J Urol.* 1997; 157:1197–1203. [PubMed: 9120901]
26. Williams JC Jr, Saw KC, Paterson RF, et al. Variability of renal stone fragility in shock wave lithotripsy. *Urology.* 2003; 61:1092–1096. [PubMed: 12809867]
27. Eisenmenger W. The mechanisms of stone fragmentation in eswl. *Ultrasound Med Biol.* 2001; 27:683–693. [PubMed: 11397533]
28. Matlaga BR, McAteer JA, Connors BA, et al. Potential for cavitation-mediated tissue damage in shockwave lithotripsy. *J Endourol.* 2008; 22:121–126. [PubMed: 18315482]
29. Connors BA, McAteer JA, Evan AP, et al. Evaluation of shock wave lithotripsy injury in the pig using a narrow focal zone lithotripter. *BJU Int.* 2012; 110:1376–1385. [PubMed: 22519983]
30. Evan AP, McAteer JA, Connors BA, et al. Independent assessment of a wide-focus, low-pressure electromagnetic lithotripter: Absence of renal bioeffects in the pig. *BJU Int.* 2008; 101:382–388. [PubMed: 17922871]

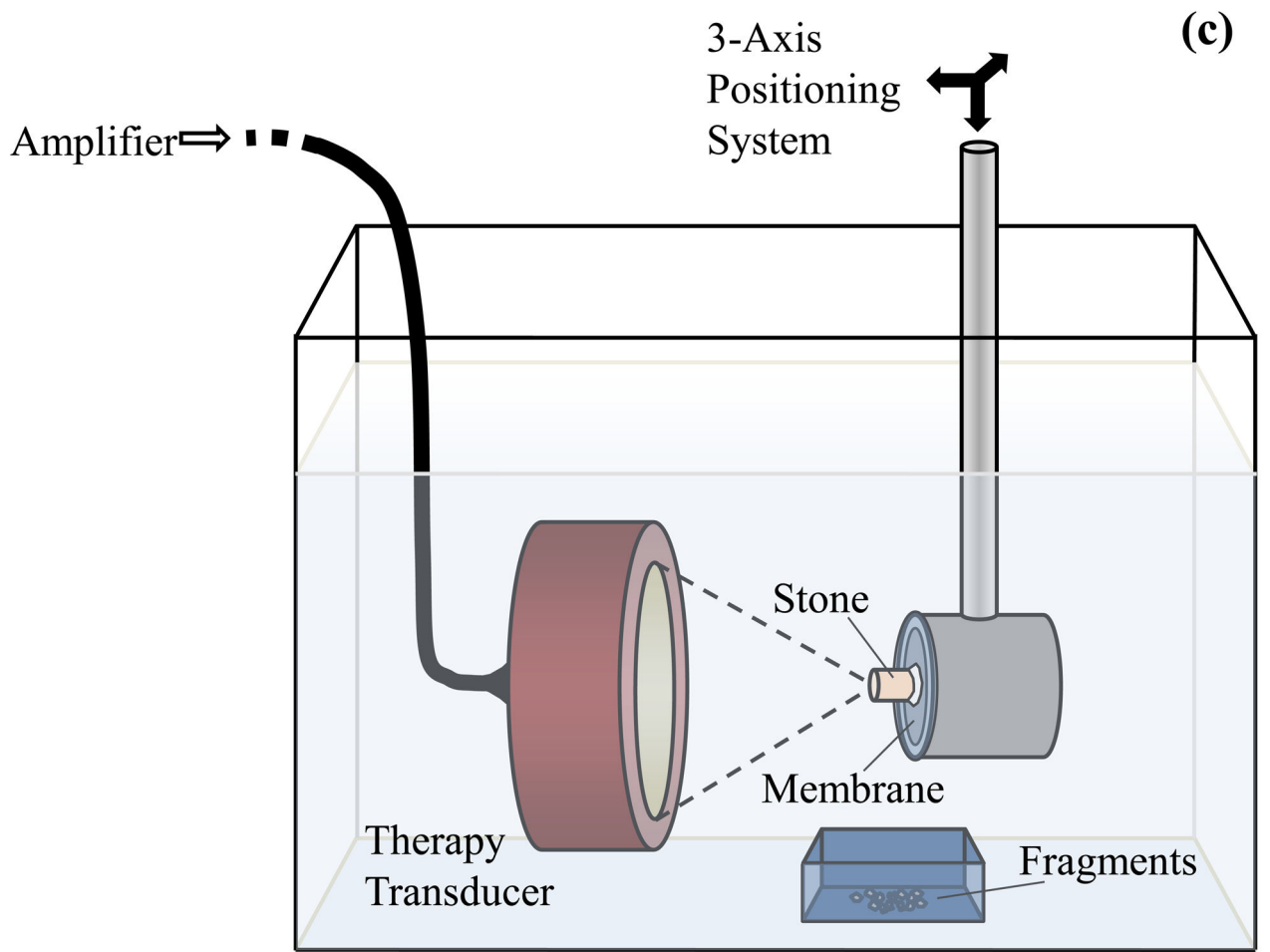
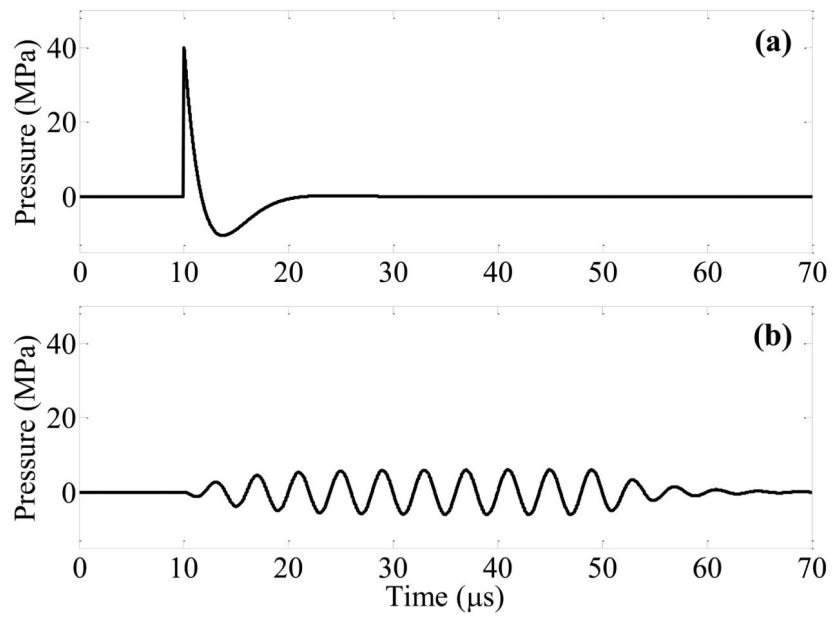
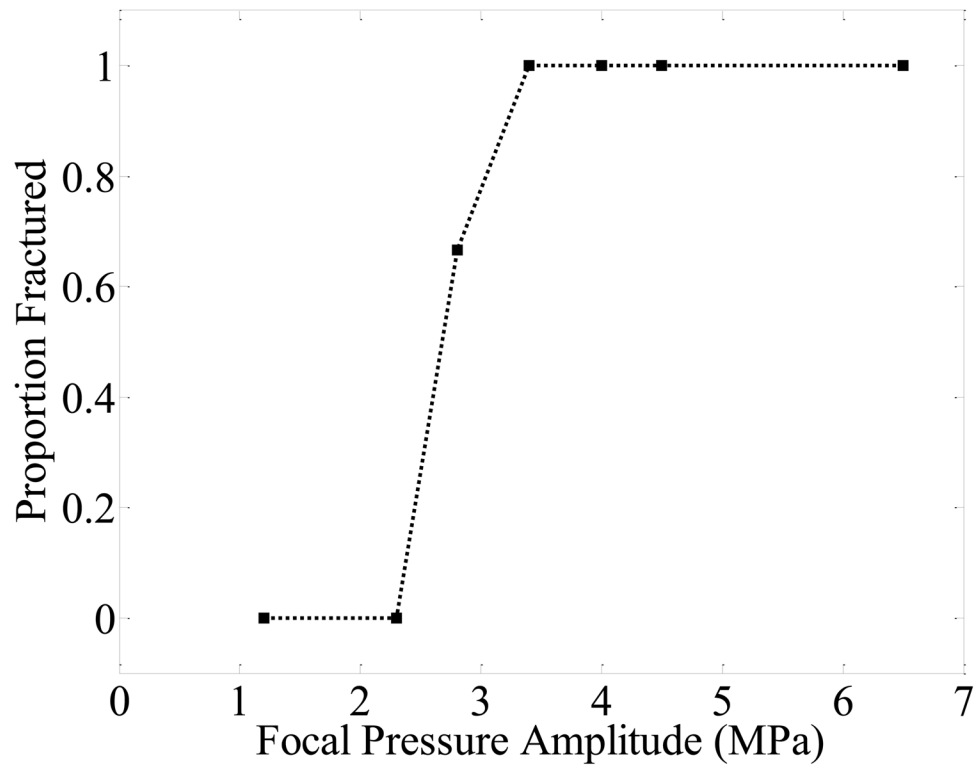


Figure 1.

Modeled focal pressure waveforms for a lithotripsy shock wave (a) and ultrasound burst wave (b). The waveform in (a) approximates the shock from a Dornier HM3 lithotripter, while the burst wave in (b) corresponds with the highest pressure amplitude ( $p_a = 6.5$  MPa) applied in this study. The experimental setup for exposure of stones to burst waves is shown in (c). A focused ultrasound transducer was placed in water tank, and the stone was aligned with the focus using a motorized 3-axis positioning system. The transducer was driven by an amplifier to expose the stone to ultrasound bursts. Fragments were collected in a small container positioned below the stone.



**Figure 2.** Proportion of artificial stones containing fractures after exposure to 60,000 bursts as a function of focal pressure amplitude. At each pressure level,  $n = 3$  stones were tested.



**Figure 3.**

Photographic sequence of an artificial stone during exposure to 170 kHz bursts with  $p_f = 6.5$  MPa over 8 minutes. Ultrasound (US) burst waves are incident on the stone from the left. The photograph to the right shows the fragments generated after 8 minutes of exposure. The scale bar is 1 cm.

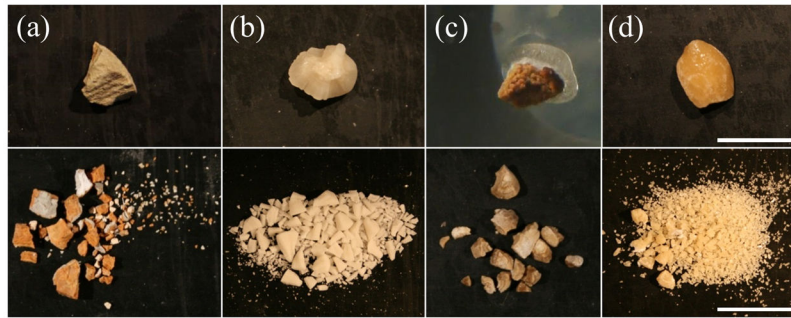


**Figure 4.** Images of uric acid (a), struvite (b), COM (c), and cystine (d) stones. The top images show the stone before 170-kHz burst wave exposure, and the bottom shows after treatment. The scale bars in (d) are 1 cm. All images have identical scales.

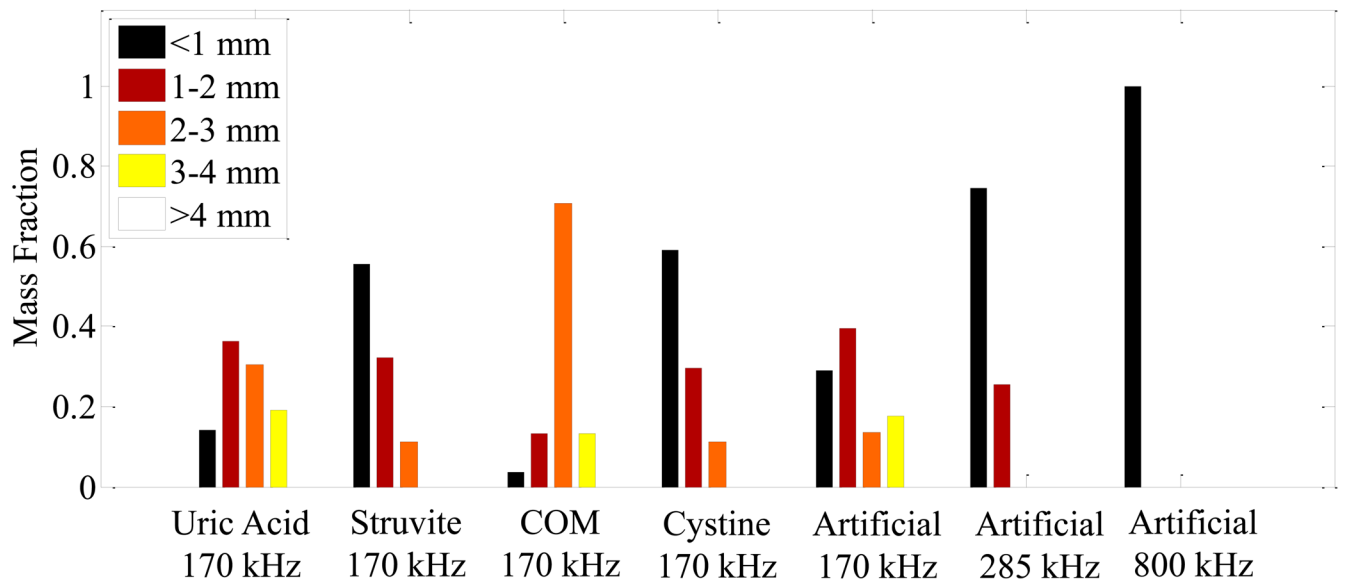


**Figure 5.** Size distribution of fragments post-exposure measured by serial sieving of fragments. The left 4 groups show the size distribution of fragments for natural stones treated with 170 kHz bursts, while the right 3 groups show the size distribution of artificial stones treated with 170 kHz, 285 kHz, and 800 kHz bursts. All measurements are mean values for stones treated in each category. COM = calcium oxalate monohydrate.

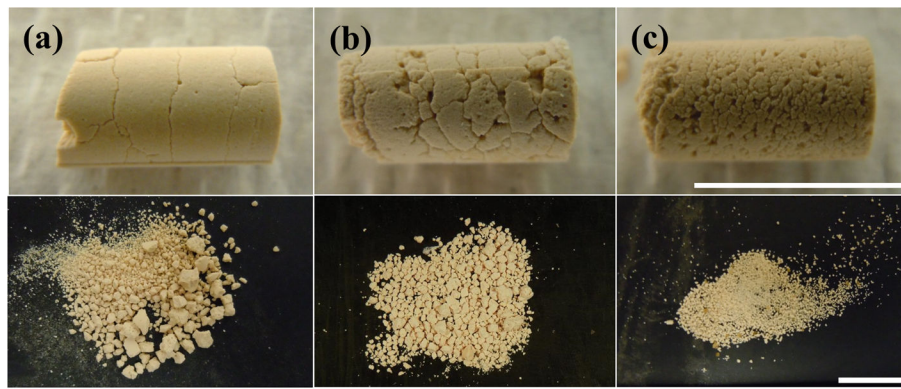


**Figure 6.**

Photographs of fractures (top) and fragments (bottom) generated for stones treated with 170 kHz (a), 285 kHz (b), and 800 kHz (c) bursts with similar peak pressure amplitude applied to the stone. Increased ultrasound frequency resulted in stone surface fractures closer together and decreased fragment size. Bursts were incident from the left side of the stone in each of the photographs. The scale bars for the top and bottom rows are both 1 cm.

SWL = Shock Wave Lithotripsy

BWL = Burst Wave Lithotripsy

COM = Calcium Oxalate Monohydrate

**Table 1**

Geometric characteristics and -6dB focal pressure beamwidths for the three transducers used in the study.

Center Frequency (kHz)	Aperture (mm)	Focal Length (mm)	Axial Beamwidth (mm)	Lateral Beamwidth (mm)
170	80	54	32.4	7.6
285	100	75	42.0	5.6
800	147	140	17.0	2.6

Author Manuscript

Author Manuscript

Author Manuscript

Author Manuscript

**Table 2**

Summary of experiments performed in the present study.

<b>Experiment Description</b>	<b>Stone Type</b>	<b>Variable</b>	<b>Measurements</b>
1 Determine pressure threshold for stone fracture by bursts	Artificial	Pressure amplitude	Stone fracture yes/no
2 Determine effect of stone composition on fragmentation	Artificial + Natural	Stone composition	Time to fragment + fragment size distribution
3 Determine effect of ultrasound frequency on fragmentation	Artificial	Ultrasound frequency	Fragment size distribution

Author Manuscript

Author Manuscript

Author Manuscript

Author Manuscript